Histol Histopathol (2023) 38: 1145-1156

Histology and Histopathology
From Cell Biology to Tissue Engineering

ORIGINAL ARTICLE Open Access

Circ-CCS regulates oxaliplatin resistance via targeting miR-874-3p/HK2 axis in colorectal cancer

Xiaofeng Qiu[1]*, Qihua Xu[2]*, Bingling Liao[2], Sheng Hu[1], Ying Zhou[2] and Huijun Zhang[2]

[1]Department of General Surgery and [2]Department of Gastroenterology, Seventh People's Hospital of Shanghai University of Traditional Chinese Medicine, Shanghai, China

*Xiaofeng Qiu and Qihua Xu contributed equally to this work

Summary. Background. Colorectal cancer (CRC) is a malignancy that threatens the patient's life. Previous reports showed that circular RNAs (circRNAs) can affect CRC development. Herein, we demonstrated the characters of circular RNA copper chaperone for superoxide dismutase (circ-CCS) in CRC tissues and cells.

Methods. Circ-CCS, CCS mRNA, microRNA-874-3p (miR-874-3p) and hexokinase 2 (HK2) were indicated by qRT-PCR and western blot in CRC. The cell roles were examined. Additionally, the interaction between miR-874-3p and circ-CCS or HK2 was forecasted by the bioinformatics method and assessed by dual-luciferase reporter assay. Finally, the mouse test was implemented to demonstrate the effect of circ-CCS *in vivo*.

Results. Circ-CCS and HK2 were increased, whereas miR-874-3p was diminished in CRC. Circ-CCS lack subdued the IC_{50} value of oxaliplatin, cell proliferation, migration, invasion and glycolysis metabolism in CRC cells, while it endorsed cell apoptosis. Furthermore, miR-874-3p was validated as having a tumor repressive effect in CRC cells by restraining HK2. The results also showed that HK2 could regulate the development of CRC. In mechanism, circ-CCS targeted miR-874-3p to control HK2. In addition, circ-CCS knock-down also attenuated tumor growth in mice.

Conclusion. Circ-CCS expedited CRC through miR-874-3p/HK2.

Key words: Colorectal cancer, circ-CCS, miR-874-3p, HK2

Corresponding Author: Ying Zhou, Seventh People's Hospital of Shanghai University of Traditional Chinese Medicine, No358, Datong Road, Pudong New Area, Shanghai City, 200137, PR China. e-mail: drzhouying226@163.com or Huijun Zhang, MM, Seventh People's Hospital of Shanghai University of Traditional Chinese Medicine, No358, Datong Road, Pudong New Area, Shanghai City, 200137, PR China. e-mail: 15301637256@163.com

www.hh.um.es. DOI: 10.14670/HH-18-565

Introduction

Colorectal cancer (CRC) is a malignancy in the Nordic countries and its incidence is increasing year by year in young patients (Thanikachalam and Khan, 2019). Among the factors associated with changes in CRC incidence, low socioeconomic status was most strongly associated with the risk of developing CRC (Cheng et al., 2011). Approximately 20% of patients with CRC present with metastatic disease. CRC is easily metastasized through lymph nodes, blood, and peritoneum to regional lymph nodes, lung, and peritoneum (Thanikachalam and Khan, 2019). Over the past 10-15 years, screening, surgery, and chemotherapy have further reduced the incidence of CRC and improved patient outcomes, but the results remain unsatisfactory (Haraldsdottir et al., 2014). Therefore, the discovery of potential targets has always been an urgent problem in the treatment of CRC.

Circular RNAs (circRNAs) are a class of RNAs, which have no 5'-caps and 3'-tails and can stably exist in plentiful types of organisms (Ambros, 2004; Garzon et al., 2010). An increasing body of research reveals that circRNAs have imperative effects in numerous cancers (Greene et al., 2017; Sheng et al., 2018). Circular RNA copper chaperone for superoxide dismutase (circ-CCS) supports the development of lung cancer (Yuan et al., 2021). In addition, circHIPK3 and circ_0000392 promote CRC growth and metastasis (Zeng et al., 2018; Xu et al., 2020). Hsa_circRNA_103809 takes part in regulating cell migration in CRC (Bian et al., 2018). Nevertheless, the detailed character of circ-CCS in CRC is still unclear.

MicroRNAs (miRNAs) can participate in regulating many cell developments (Ambros, 2004; Garzon et al., 2010). For example, miR-874-3p inhibits cell migration in osteosarcoma (Liu et al., 2020). MiR-874-3p prevents epithelial ovarian cancer malignancy (Xia et al., 2018). Besides, miR-338-3p suppresses the proliferation of CRC (Zou et al., 2018). Moreover, miR-154-5p regulates cell growth in CRC (Xu et al., 2018). Nevertheless, our

comprehending of their specific effects in CRC remains restricted and needs further study.

There is growing evidence that hexokinase 2 (HK2) plays an essential role in glycolysis and cell survival. HK2 is an important target in glucose metabolism and is involved in regulating rate-limiting steps in the glycolysis pathway (Ros and Schulze, 2013). It has been testified that HK2 is up-regulated in liver cancer tissues and affects the prognosis of patients. At the same time, HK2 also plays an important role in autophagy (Roberts et al., 2014). Meanwhile, HK2 takes part in the progress of Cervical Cancer (Liu et al., 2019). Nevertheless, the behavior of HK2 in CRC cells, as well as the progression of CRC, is still unclear.

In brief, we revealed the purpose of circ-CCS in CRC cells. Circ-CCS may expedite CRC tumor enlargement. Our conclusions may be a novel perception to the growth of CRC.

Materials and methods

Clinical samples

The test was examined by Seventh People's Hospital of Shanghai University of Traditional Chinese Medicine. Thirty-Seven pairs of CRC tissues and corresponding normal tissues were collected from Seventh People's Hospital of Shanghai University of Traditional Chinese Medicine. Meanwhile, nineteen pairs of oxaliplatin-resistant and oxaliplatin-sensitive colorectal cancer tissues were derived from CRC patients with signed informed consent.

Cell lines and transfection

In this paper, cell lines used were LoVo, SW620, SW480, and HCT-116 with NCM460 as control. All cells were obtained from JCRB cell bank (Osaka, Japan) and cultured with 10% FBS in an environment with 5% CO_2 at 37°C. SW480/OXA and HCT-116/OXA cells were established by treating oxaliplatin (Sigma-Aldrich, St. Louis, MO, USA) into SW480 and HCT-116 cells from 1/50 IC_{50} content for more than 6 months in a 10% DMEM medium.

The si-circ-CCS, sh-circ-CCS, the control (si-NC and sh-NC), miR-874-3p mimics, miR-874-3p inhibitors and controls HK2 overexpression (HK2) and control plasmid (pcDNA) were attained from Ribobio (Guangzhou, China). Lipofectamine 2000 (Sigma) was conducted in transfection.

QRT-PCR and RNase R assay

TRIzol (Sigma) was conducted to RNA preparation. Following, the RNA was enforced to implement reverse transcription and qRT-PCR in agreement with the prior information (Gai et al., 2020). GAPDH and U6 were employed to standardize RNA levels. All data were reckoned by $2^{-\Delta\Delta Ct}$ system. RNase R (Sigma) was conducted to mark the cyclic structure of circ-CCS. The total RNA with or without RNase R treatment was used for qRT-PCR to detect the level of circ-CCS and linear CCS. The primer sequences are shown in Table 1.

Western blot

The technique of western blot was used as in the past (Hou and Zhang, 2021). The antibodies were as follows: anti-HK2 (ab273721; 1:1,000; Abcam, Cambridge, MA, USA), anti-MRP1 (ab260038; 1:1000; Abcam) and anti-β-actin (ab8227; 1:1000; Abcam).

CCK8 assay

SW480/OXA and HCT-116/OXA (2.0×10^3/well) cells were planted into 96-well plates. CCK8 (Sigma) was employed in agreement with the directions. The half-maximal inhibitory concentration (IC_{50}) was assessed at 450 nm and the identical technique was utilized to authenticate the cell viability.

Cell proliferation assay

The Cell-Light™ EdU kit (Ribobio) was conducted to assess the cell proliferation following instructions

Flow cytometry assay

At 24h post-transfection, 2×10^4 SW480/OXA and HCT-116/OXA cells were planted into 6-well plates. Then, an Annexin V-FITC/PI kit (Sigma) was implemented on the base of the guide. A Flow cytometer

Table 1. Primers for PCR.

Name	Primers for PCR (5'-3')	
circ-CCS	Forward	GACACAGCAAAGGAAGGGTC
	Reverse	CAACCTCCACCTCCTGAGTT
HK2	Forward	GGTGGACAGGATACGAGAAAAC
	Reverse	ACATCACATTTCGGAGCCAG
miR-874-3p	Forward	GCCGAGCTGCCCTGGCCCGAGGG
	Reverse	CATTTTTTCCACTCCTCTTCTCTC
GAPDH	Forward	TCCCATCACCATCTTCCAGG
	Reverse	GATGACCCTTTTGGCTCCC
miR-198	Forward	GCCGAGGGTCCAGAGGGGAGA
	Reverse	CTCAACTGGTGTCGTGGA
miR-197-3p	Forward	GCCGAGTTCACCACCTTCTCCA
	Reverse	CTCAACTGGTGTCGTGGA
miR-383-5p,	Forward	GCCGAGAGATCAGAAGGTGATT
	Reverse	CTCAACTGGTGTCGTGGA
miR-876-3p	Forward	GCCGAGTGGTGGTTTACAAAGUA
	Reverse	CTCAACTGGTGTCGTGGA
U6	Forward	CTCGCTTCGGCAGCACATATACT
	Reverse	ACGCTTCACGAATTTGCGTGTC
CCS	Forward	GGGAACTATTGACGGCCTGG
	Reverse	GTCAGCATCAGCACGGACAT

was applied to assess the count of apoptotic cells.

Transwell assay

SW480/OXA and HCT-116/OXA cells were supplemented into the higher chambers with Matrigel (Corning, Corning, NY, USA). Simultaneously, the culture medium with 10% FBS occupied the inferior chambers. After 24h, the invasion cells were dyed and photographed through a microscope.

Wound-healing assay

At 24h post-transfection, SW480/OXA and HCT-116/OXA cells were plated on the 6-well plates. In simple terms, the cells were scratched by a germ-free pipette tip, then treated with FBS-free media for 24h. Next, under a microscope, the distances were measured.

Glycolysis metabolism assay

SW480/OXA and HCT-116/OXA (2.5×10^5 cells/well) were planted into 6-well plates. The Glucose Assay Kit and L-Lactate Assay Kit (Sigma) were utilized as stated by the guidelines.

Dual-luciferase reporter assay

The connection between miR-874-3p and circ-CCS or HK2 was estimated by circinteractome and starbase. The wild and mutant circ-CCS or HK2 were manufactured by Ribobio (WT-circ-CCS, WT-HK2 3'UTR or MUT-circ-CCS, MUT-HK2 3'UTR). The luciferase activity was scrutinized.

Xenograft models

The experiments abided by the guidance of the Animal Care and Use Committee of Seventh People's Hospital of Shanghai University of Traditional Chinese Medicine. All 36 nude mice (5 weeks; 18-22 g; female) were obtained from Shanghai Laboratory Animal Company (SLAC, Shanghai, China). These mice were divided into four groups (sh-NC + PBS, sh-NC + OXA, sh-circ-CCS + PBS and sh-circ-CCS + OXA, N=8 per group). Then, 4×10^6 cells after transfection were injected into the mice, which were treated with oxaliplatin (20 mg/kg) after 3 days. After 25 days of oxaliplatin treatment, mice were euthanized and the level of circ-CCS was assessed. Tumor volume=length × width^2 × 0.5.

IHC assay

The Ki67 (ab92742; 1:1,000; Abcam) and MMP2 (ab86607; 1:1,000; Abcam) contents in tumor were quantified by utilizing IHC. The precise scheme is as per the explanation of Ma et al. (2021). In the end, the slides were photographed.

Statistical assay

We executed our investigation in triplicate. Pearson's correlation analysis was utilized to speculate the correlation. Student's t-test or ANOVA was implemented through SPSS. $P<0.05$ was noteworthy.

Results

Circ-CCS was expedited in CRC

GSE126094 microarray analysis verified that circ-CCS presented high expression in CRC (Fig. 1A,B). Hence, the levels of circ-CCS were augmented in CRC tissues (Fig. 1C). Moreover, the relationship between circ-CCS expression and clinicopathologic features of CRC patients are presented in Table 2. We found higher levels of circ-CCS in patients with more advanced tumors or lymph node metastases. Furthermore, our information submitted that circ-CCS was enhanced in four CRC cell lines (LoVo, SW620, SW480 and HCT-116) relative to the control cell line (NCM460) and was greatly increased in oxaliplatin-resistant tissues (n=19) relative to oxaliplatin-sensitive tissues (n=19) (Fig. 1D,E). We detected the IC_{50} value of oxaliplatin in SW480, HCT-116, SW480/OXA and HCT-116/OXA cells. Figure 1F demonstrates that the IC_{50} of cisplatin was augmented in SW480/OXA and HCT-116/OXA cells versus that in SW480 and HCT-116 cells, which signposted that oxaliplatin resistant SW480 and HCT-116 cells were efficaciously established. Next, the expressions of circ-CCS in oxaliplatin-resistant CRC cell lines (SW480/OXA and HCT-116/OXA) were further explored. Similarly, higher expression of circ-CCS was discovered in oxaliplatin-resistant CRC cells in

Table 2. Relationship between circ-CCS expression and clinicopathologic features of colorectal cancer patients.

Characteristics	n=37	circ-CCS expression		P value[a]
		Low(n=18)	High(n=19)	
Gender				0.1914
Female	17	6	11	
Male	20	12	8	
Age (years)				0.1939
≤60	18	11	7	
>60	19	7	12	
TNM grade				0.0081*
I+II	16	12	4	
III+IV	21	6	15	
Lymph node metastasis				0.0069*
Positive	23	7	16	
Negative	14	11	3	
Tumor size				0.0029*
≤5 cm	17	13	4	
>5 cm	20	5	15	

TNM, tumor-node-metas-tasis; *: $P<0.05$ [a]: Chi-square test.

comparison with their parental cells SW480 and HCT-116 (Fig. 1G). In addition to this, to further confirm the structure of circ-CCS, an RNase R enzyme (a highly processive 3' to 5' exoribonuclease) assay was conducted to distinguish the structure of circ-CCS and linear CCS in SW480/OXA and HCT-116/OXA cell lines. As displayed in Figure 1H,I, circ-CCS was resistant to RNase R treatments, whereas linear CCS was dramatically degraded. These outcomes exposed that circ-CCS was upregulated in CRC, particularly in oxaliplatin-resistant tissues and cells, suggesting that circ-CCS might take effects on oxaliplatin resistance in CRC.

Silencing circ-CCS promotes cell apoptosis, whereas this restrains the IC_{50} value of oxaliplatin and cell proliferation.

Firstly, circ-CCS level was limited in SW480/OXA and HCT-116/OXA cells by si-circ-CCS (Fig. 2A). Next, the results showed that the knockdown of circ-CCS decreased the IC_{50} value of oxaliplatin (Fig. 2B). In addition, silence of circ-CCS diminished cell proliferation (Fig. 2C,D). Besides, circ-CCS down-regulation enhanced cell apoptosis in SW480/OXA and HCT-116/OXA cells (Fig. 2E). Our results indicate that circ-CCS lack might promote cell apoptosis, whereas it

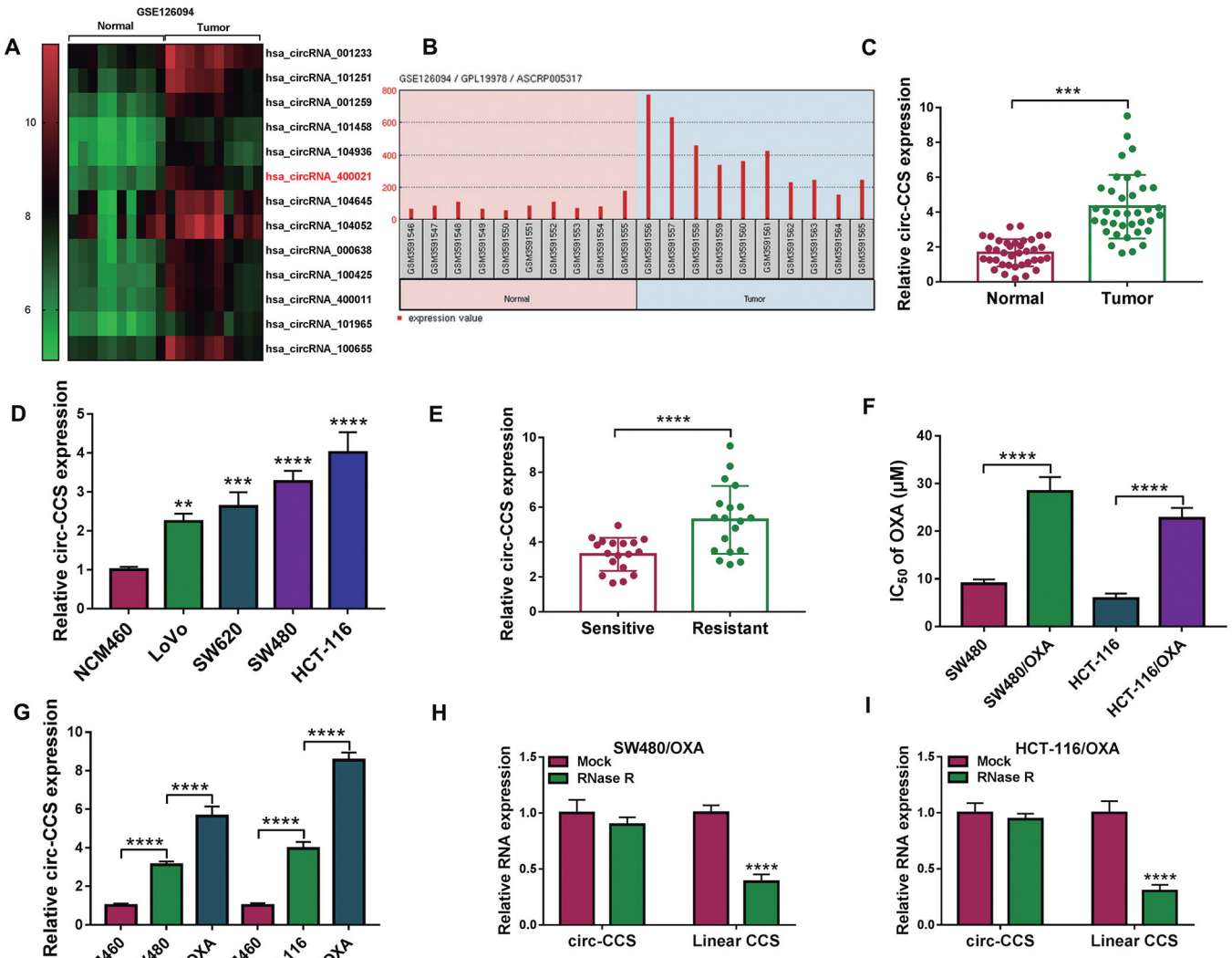

Fig. 1. Circ-CCS expression was elevated in CRC. **A, B.** GSE126094 microarray analyzed the circRNA expression profiling between CRC tissues and adjacent normal tissues. **C.** The circ-CCS levels were quantified. **D.** The contents of circ-CCS in NCM460, LoVo, SW620, SW480 and HCT-116 cells were determined. **E.** The expression of circ-CCS in CRC oxaliplatin-resistant tissues (n=19) and oxaliplatin-sensitive tissues (n=19) were measured. **F.** The IC_{50} of OXA was examined. **G.** The circ-CCS levels in CRC cells. **H, I.** The relative levels of circ-CCS and linear CCS mRNA were examined. $^{**}P<0.01$, $^{***}P<0.001$, $^{****}P<0.0001$.

restrains the IC_{50} value of oxaliplatin and cell proliferation.

Silencing circ-CCS restrained migration, invasion and glycolysis metabolism in CRC cells

Subsequently, the knockdown of circ-CCS repressed invasion and migration of SW480/OXA and HCT-116/OXA cells (Fig. 3A,B). Meanwhile, the level of MRP1, a drug-resistant associated protein, was decreased by si-circ-CCS (Fig. 3C). Next, the knockdown of circ-CCS significantly repressed glycolysis metabolism in SW480/OXA and HCT-116/OXA cells (Fig. 3D,E). Figure 3F shows that circ-CCS expression was notably enhanced in SW480/OXA and HCT-116/OXA cells with circ-CCS compared to the pCD5-ciR group. 2-Deoxy-D-glucose (2-DG) is a glucose analogue and an inhibitor of glucose metabolism. We discovered that circ-CCS could enhance the IC_{50} value of oxaliplatin, but this effect was lessened by 2-DG (Fig. 2G). Our views suggested that silencing circ-CCS restrained migration, invasion and glycolysis metabolism in CRC cells.

Circ-CCS downregulation impeded tumor growth in vivo

The data specified that the circ-CCS level was constrained in HCT-116/OXA cells transfected with sh-circ-CCS compared to the sh-NC group (Fig. 4A). As shown in Figure 4B,C, oxaliplatin treatment suppressed

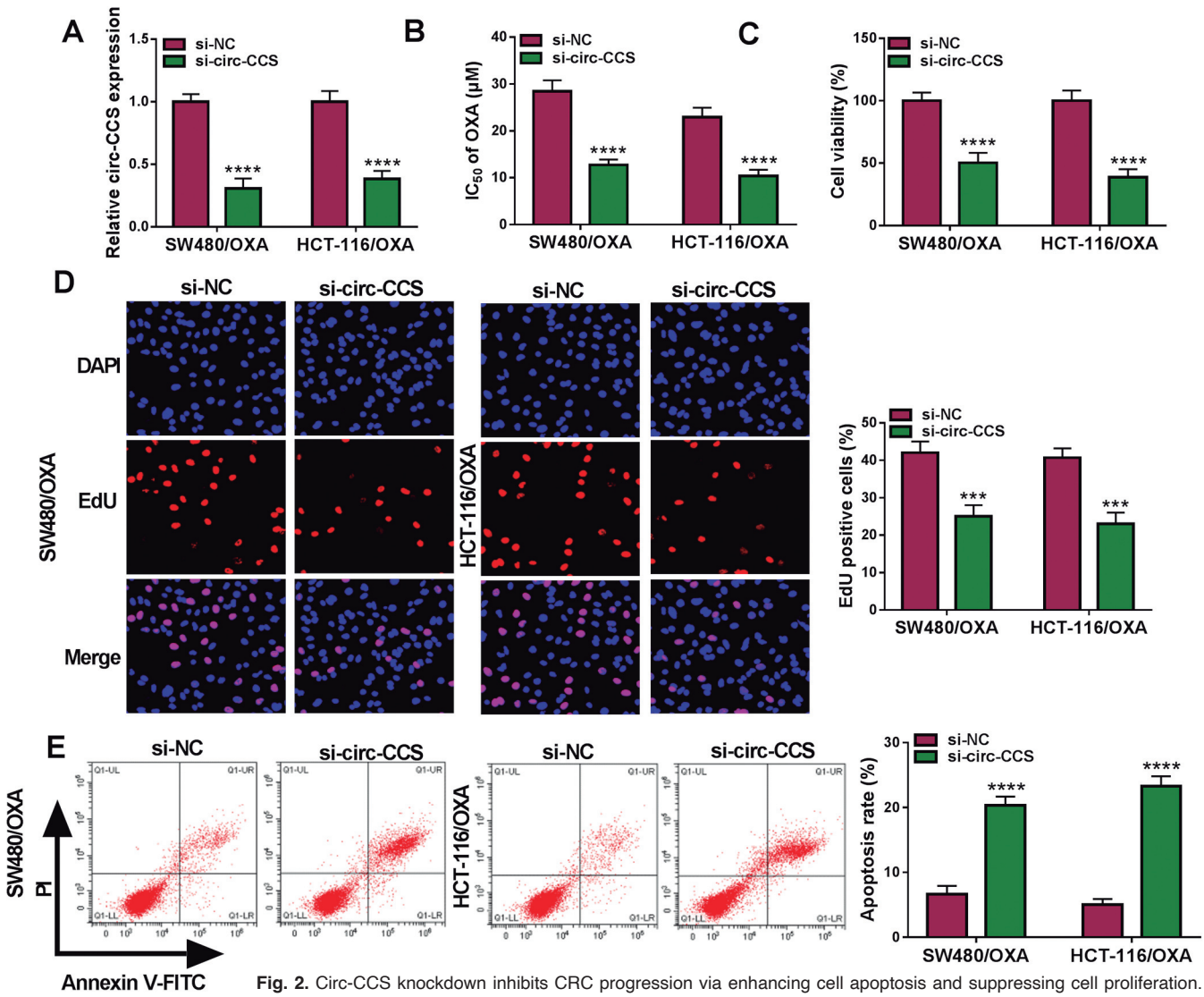

Fig. 2. Circ-CCS knockdown inhibits CRC progression via enhancing cell apoptosis and suppressing cell proliferation. **A.** The circ-CCS level was quantified in SW480/OXA and HCT116/OXA cells transfected with si-circ-CCS or si-NC. **B.** The IC_{50} of OXA in SW480/OXA+si-NC, SW480/OXA+si-circ-CCS, HCT-116+si-NC, HCT-116+si-circ-CCS cells. **C, D.** The cell proliferation was demonstrated. **E.** The apoptosis of CBC cells. ***P<0.001, ****P<0.0001.

tumor volume and weight, and circ-CCS lack improved these influences. To inspect the influences between circ-CCS downregulation and oxaliplatin treatment on circ-CCS levels, qRT-PCR was accomplished to elucidate that circ-CCS deletion blocked circ-CCS expression, and the levels of circ-CCS were also subdued by sh-circ-

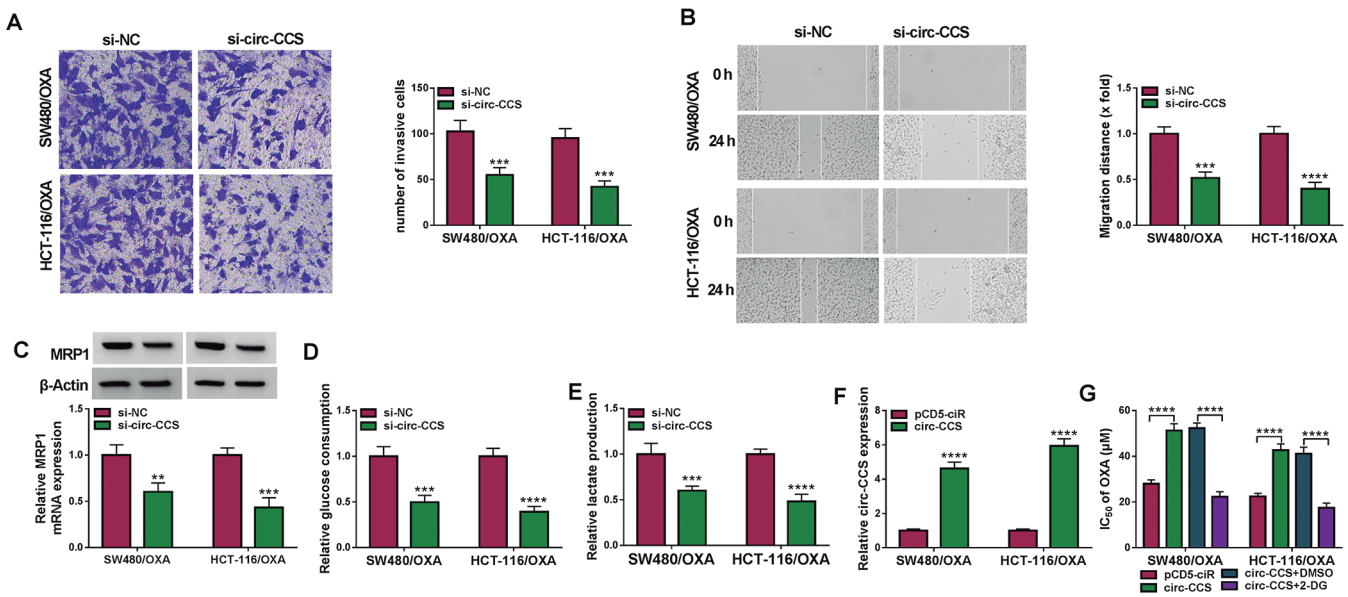

Fig. 3. Circ-CCS knockdown inhibits CRC progression via suppressing migration, invasion and glycolysis metabolism. **A, B.** The cell invasion and migration was measured. **C.** The MRP1 level was quantified. **D, E.** The levels of glucose metabolism. **F.** The expression of circ-CCS was determined by qRT-PCR. **G.** The IC_{50} of OXA was examined by CCK8 assay. $^{**}P<0.01$, $^{***}P<0.001$, $^{****}P<0.0001$.

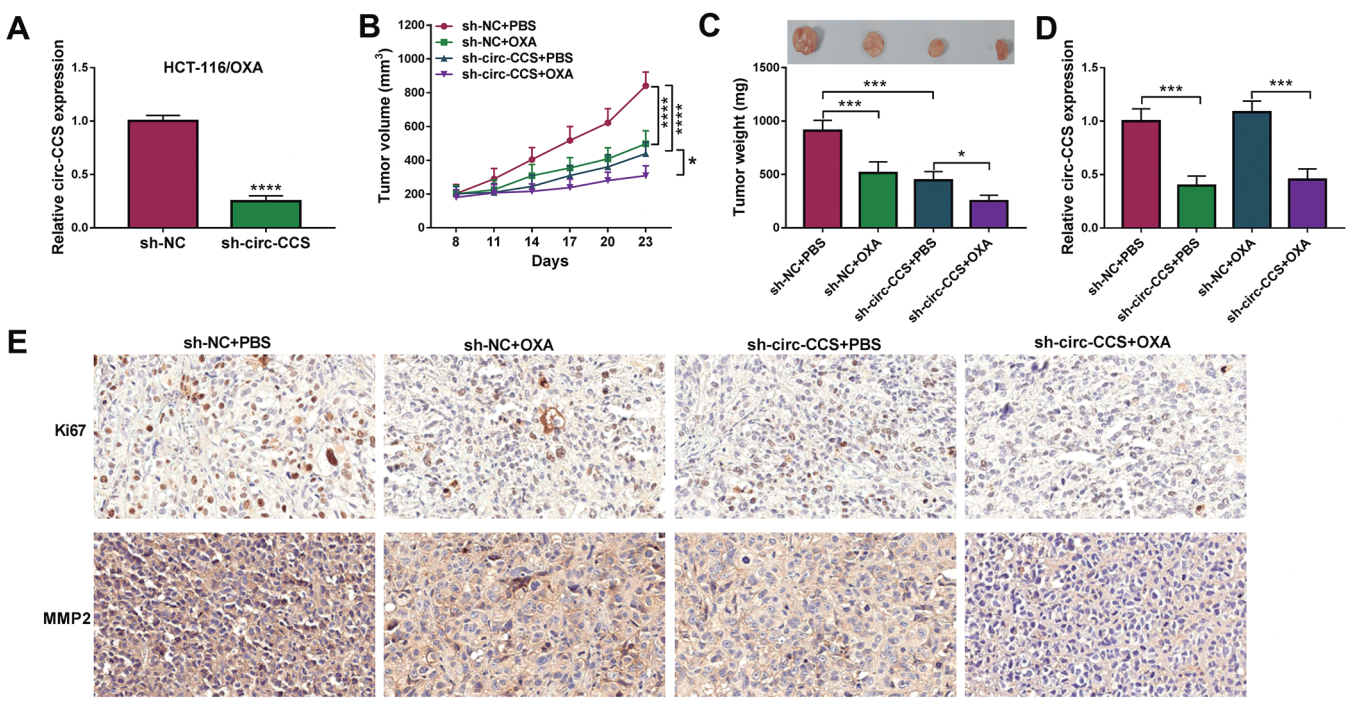

Fig. 4. Circ-CCS knockdown diminished tumor growth. **A.** The circ-CCS level was examined. **B, C.** Tumor volume and weight were measured. **D.** The circ-CCS level was quantified. **E.** The Ki67 and MMP2 levels were examined. $^{*}P<0.05$, $^{***}P<0.001$, $^{****}P<0.0001$.

CCS after oxaliplatin exposure (Fig. 4D). Besides, the levels of MMP2 and Ki67 were decreased by oxaliplatin treatment, and circ-CCS lack improved these influences (Fig. 4E). Overall, circ-CCS deficiency restrained tumor growth and strengthened OXA sensitivity *in vivo*.

MiR-874-3p targeted circ-CCS

We made a prediction through the circinteractome website, and combined with literature research to find miRNA with low expression and tumor growth inhibition in colorectal cancer. Possible targeted miRNA included miR-198, miR-197-3p, miR-383-5p, miR-876-3p, miR-874-3p. Then, it was found that the content of miR-874-3p changed the most by transfection of si-circ-CCS. Therefore, miR-874-3p was used as a target for research (Fig. 5). Circinteractome was conducted to forecast that miR-874-3p is a target of circ-CCS (Fig. 6A). Moreover, the miR-874-3p content was amplified by miR-874-3p mimic (Fig. 6B). The luciferase activity was diminished in in SW480/OXA and HCT-116/OXA cells with cotransfection of WT-circ-CCS and miR-874-3p versus miR-NC groups. Meanwhile, the information demonstrated that miR-874-3p level was markedly reduced in oxaliplatin resistant tissues (n=19) versus that in oxaliplatin sensitive tissues (n=19) (Fig. 6E). Besides, Pearson's correlation analysis indicated that miR-874-3p level was negatively correlated with circ-CCS in CRC tissues (Fig. 6F). Next, the expressions of miR-874-3p in oxaliplatin-resistant CRC cell lines (SW480/OXA and HCT-116/OXA) were further explored. Similarly, lower expression of miR-874-3p was discovered in oxaliplatin-resistant CRC cells in comparison with their parental cells SW480 and HCT-116 (Fig. 6G). Furthermore, qRT-PCR was accomplished to demonstrate that circ-CCS loss increased the miR-874-3p expression, and the miR-874-3p content was repressed by circ-CCS overexpression (Fig. 6H).

Circ-CCS expedited CRC via miR-874-3p miR-874-3p was controlled in SW480/OXA and HCT-116/OXA cells with anti-miR-874-3p versus the anti-miR-NC group (Fig. 7A). SW480/OXA and HCT-116/OXA cells were transfected with si-circ-CCS and si-circ-CCS + anti-miR-874-3p, with si-NC and si-circ-CCS + anti-miR-NC as the control. We discovered that circ-CCS loss augmented the level of miR-874-3p in SW480/OXA and HCT-116/OXA cells, while this consequence was lessened by miR-874-3p inhibitor (Fig. 7B). For further research on the effects between circ-CCS and miR-874-3p on CRC progression, we discovered that downregulation of circ-CCS lessened the IC_{50} value of oxaliplatin, but this outcome was lessened by miR-874-3p inhibitor (Fig. 7C). In addition, circ-CCS knockdown decreased the cell vitality in SW480/OXA and HCT-116/OXA cells, but this result was lessened by miR-874-3p inhibitor (Fig. 7D). Moreover, downregulated circ-CCS lessened the cell proliferation, however this

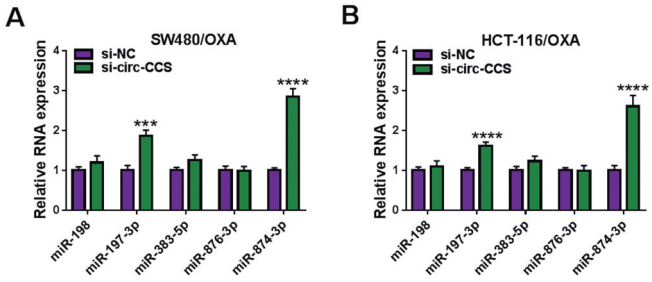

Fig. 5. The screening of the targeted miRNA. ***P<0.001, ****P<0.0001.

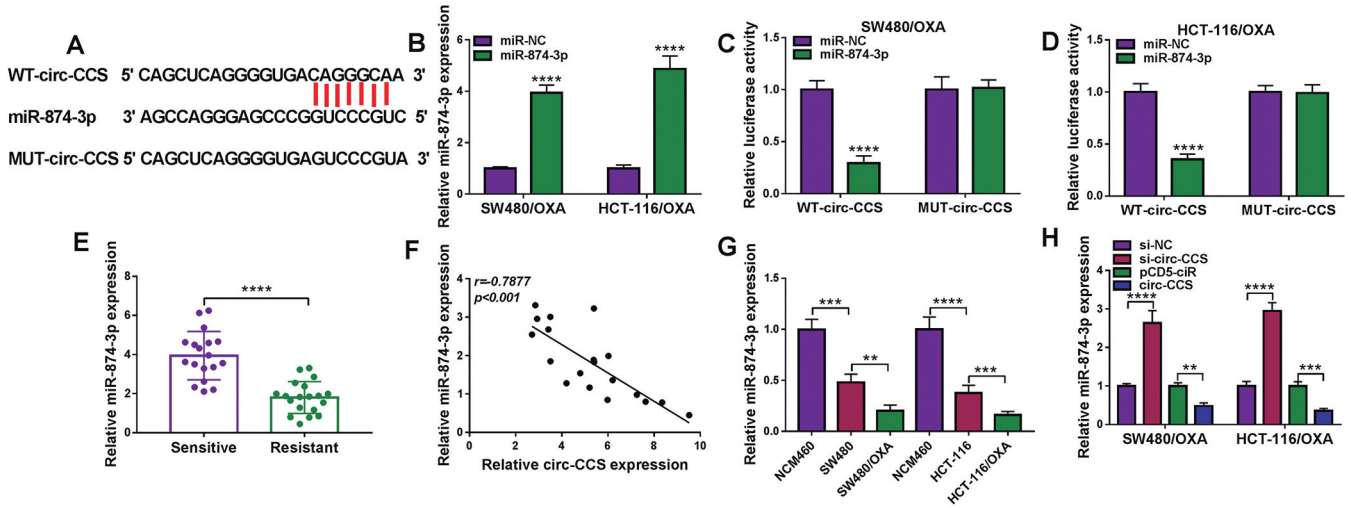

Fig. 6. Circ-CCS bound to miR-874-3p. **A.** The targeted miRNAs of circ-CCS were forecast by Circinteractome. **B.** The miR-874-3p level in CRC cells. **C, D.** The relationship of circ-CCS and miR-874-3p. **E.** The levels of miR-874-3p in CRC oxaliplatin-resistant tissues (n=19) and oxaliplatin-sensitive tissues (n=19). **F.** MiR-874-3p expression was negatively related to circ-CCS expression in CRC tissues (R=-0.7877). **G, H.** The content of miR-874-3p. **P<0.01, ***P<0.001, ****P<0.0001.

outcome was weakened by miR-874-3p inhibitor (Fig. 7E). On the other hand, flow cytometry analysis indicated that in SW480/OXA and HCT-116/OXA cells, anti-miR-874-3p partially returned the accelerated effect of circ-CCS silencing on cell apoptosis (Fig. 7F). Moreover, transwell assays and wound healing assay demonstrated that anti-miR-874-3p attenuated the destruction impacts of circ-CCS silencing on cell invasion and migration in SW480/OXA and HCT-116/OXA cells (Fig. 7G,H). The MRP1 level was reduced by circ-CCS silencing, but augmented by anti-miR-874-3p (Fig. 7I). Afterwards, the circ-CCS silencing significantly repressed glycolysis metabolism in CRC cells, but this impact was partially attenuated by miR-874-3p knockdown (Fig. 7J,K). Figure 7L showed that anti-miR-874-3p was able to enhance the IC_{50} value of oxaliplatin, but this effect was lessened by 2-DG.

MiR-874-3p targets HK2 in SW480/OXA and HCT-116/OXA cells

The target gene of miR-874-3p was predicted in this part. The binding sites were displayed (Fig. 8A). The luciferase activity of WT-HK2 3'UTR was hampered by miR-874-3p. Nevertheless, the luciferase activity of MUT-HK2 3'UTR was not altered by miR-874-3p (Fig. 8B,C). Data of gepia.cancer displayed that HK2 level was enhanced in CRC tumor tissues (N=349) versus control (N=275) (Fig. 8D). In addition, that HK2 level was markedly increased in oxaliplatin resistant tissues (n=19) versus that in oxaliplatin sensitive tissues (n=19) (Fig. 8E,G). Besides, Pearson's correlation analysis explained that HK2 level was negatively correlated with miR-874-3p in CRC (Fig. 8F). Next, the expressions of HK2 in oxaliplatin-resistant CRC cell lines (SW480/OXA and HCT-116/OXA) were further explored. Similarly, higher expression of HK2 was discovered in oxaliplatin-resistant CRC cells in comparison with their parental cells SW480 and HCT-116 (Fig. 8H). Furthermore, HK2 content was decreased by miR-874-3p mimic, whereas it was increased by anti-miR-874-3p (Fig. 8I).

MiR-874-3p repressed CRC via HK2

Transfection efficiency of HK2 was distinguished by western blot. HK2 level was increased in SW480/OXA and HCT-116/OXA cells transfected with HK2

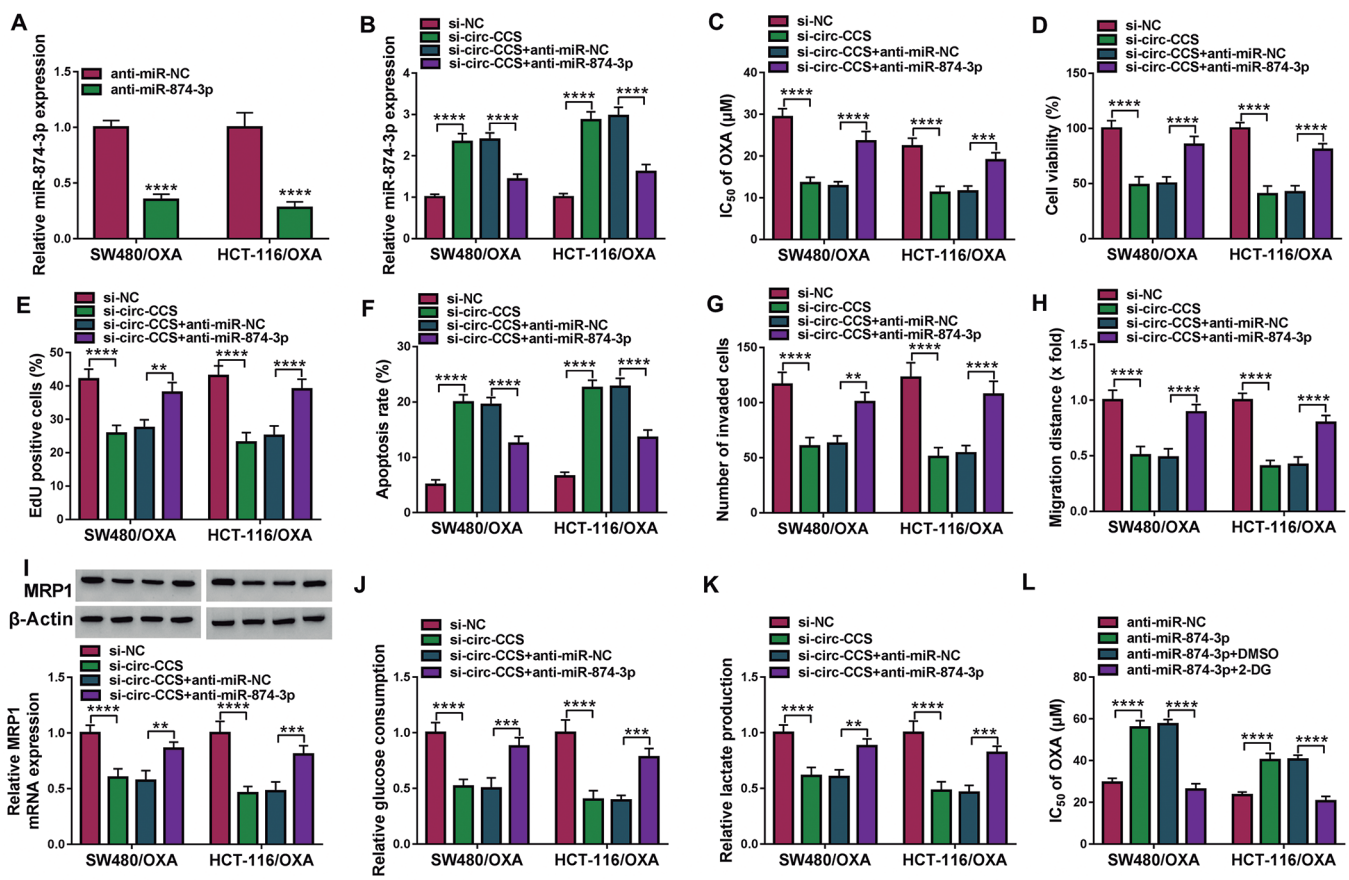

Fig. 7. Circ-CCS expedited the progression of CRC by sponging miR-874-3p. The contents of miR-874-3p in CRC cells **(A, B)**, the IC_{50} of OXA **(C)**, the OD value **(D)**, the cell proliferation **(E)**, the apoptosis **(F)**, the number of invaded cells **(G)**, the number of migration cells **(H)**, the MRP1 level **(I)**, the glucose metabolism **(J, K)**, The IC_{50} of OXA were assessed **(L)**. ***P*<0.01, ****P*<0.001, *****P*<0.0001.

compared to the pcDNA group (Fig. 9A). Then, SW480/OXA and HCT-116/OXA cells were transfected with miR-874-3p or miR-874-3p + HK2, with miR-NC or miR-874-3p + pcDNA as the control. The expression of HK2 diminished by miR-874-3p mimic in CRC cells, but this effect was partially weakened by HK2 upregulation (Fig. 9B). CCK8 assay illustrated that miR-874-3p mimic reduced the IC_{50} value of oxaliplatin and the cell vitality of SW480/OXA and HCT-116/OXA cells, whereas this influence was controlled by HK2 overexpression (Fig. 9C,D). Moreover, the outcomes of colony formation assay displayed the miR-874-3p mimic depressed cell proliferation, but this consequence was lessened by HK2 (Fig. 9E). Flow cytometry analysis, miR-874-3p facilitated cell apoptosis in SW480/OXA and HCT-116/OXA cells, and this influence was reversed by HK2 overexpression (Fig. 9F). Subsequently, the invasion and migration of SW480/OXA and HCT-116/OXA cells were repressed by miR-874-3p, but HK2 could partially obliterate these influences (Fig. 9G,H). The MRP1 level was reduced by miR-874-3p, but augmented by HK2 (Fig. 9I). Afterwards, the miR-874-3p mimic significantly repressed glycolysis metabolism in CRC cells, but this impact was partially attenuated by HK2 overexpression (Fig. 9J,K). Figure 9L shows that HK2 overexpression could enhance the IC_{50} value of oxaliplatin, but this effect was lessened by 2-DG.

Circ-CCS indirectly regulated HK2 expression via targeting miR-874-3p

In addition, the circ-CCS silencing significantly repressed the expression of HK2 in SW480/OXA and

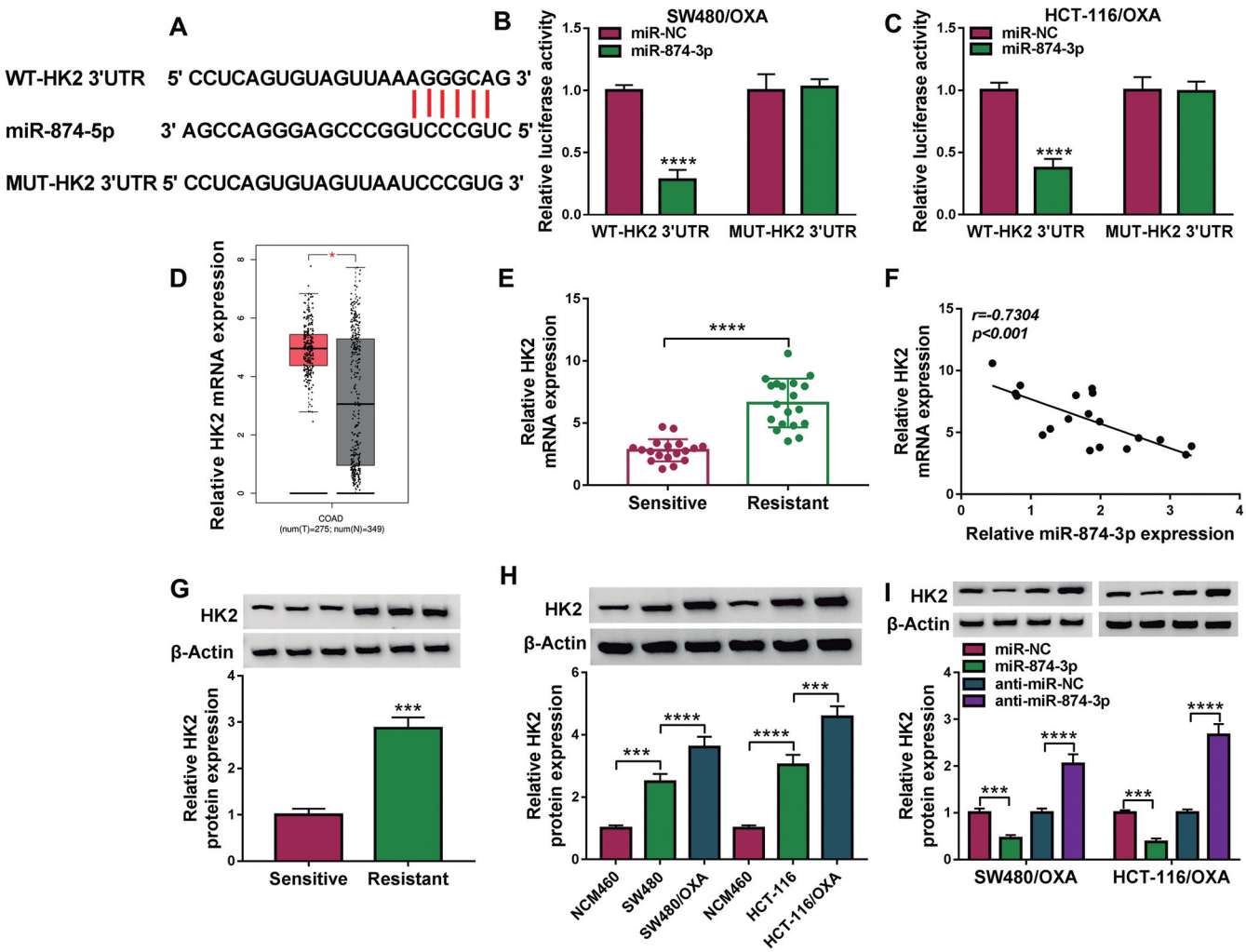

Fig. 8. MiR-874-3p targeted HK2. **A.** The binding sites of miR-874-3p and HK2. **B, C.** The connection between miR-874-3p and HK2. **D.** The contents of HK2. **E.** The HK2 levels in CRC oxaliplatin-resistant tissues (n=19) and oxaliplatin-sensitive tissues (n=19) were detected by qRT-PCR. **F.** MiR-874-3p expression was negatively linked with HK2 expression in CRC tumor tissues (R=-0.7304). **G-I.** The HK2 level was detected. ****P*<0.001, *****P*<0.0001.

HCT-116/OXA cells, but this influence was incompletely weakened by miR-874-3p inhibitor (Fig. 10A,B). In conclusion, our findings demonstrated that circ-CCS silencing hindered CRC development by targeting the miR-874-3p/HK2 axis.

Discussion

According to previous studies, although the mortality of CRC has decreased over the past few decades, the incidence of CRC continues to increase in the younger age group under 50. Among them, people's diet, nutritional status, physical activity status and other factors are closely connected with the pathogenesis and poor prognosis of CRC. Therefore, in-depth study on the molecular mechanism of CRC has important clinical and practical significance for clinical treatment.

Previous studies have discovered that some emerging circRNAs take part in the progress of CRC. A research work uncovered that circ-122 could promote glycolysis, which reduces drug sensitivity in chemically sensitive CRC cells (Wang et al., 2020). Another study reported that circCBL.11 suppresses cell proliferation in CRC (Li et al., 2019). In our paper, we indicated that circ-CCS encouraged apoptosis, while it restrains the IC_{50} value of oxaliplatin, cell proliferation, migration, invasion and glycolysis metabolism in CRC cells. In addition, our *in vivo* study further discovered that knockdown circ-CCS impaired tumor growth. CircRNAs can modulate downstream gene expression via acting as the sponges of miRNAs. Circ-122 bound to miR-122 and circCBL.11 regulated miR-6778-5p in CRC (Li et al., 2019; Wang et al., 2020). Herein, circ-CCS can increase the speed of CRC advancement by regulating miR-874-3p, which is comparable to earlier conclusions.

MiR-874-3p can adjust the development of esophageal squamous cell carcinoma, nasopharyngeal carcinoma and cervical cancer (Yuan et al., 2018; Feng et al., 2019; Liu et al., 2021). These outcomes demonstrated that miR-874-3p participated in many cancers. Herein, we displayed the inhibiting effect of miR-874-3p in CRC cell progress by regulating HK2. The outcomes corroborated that miR-874-

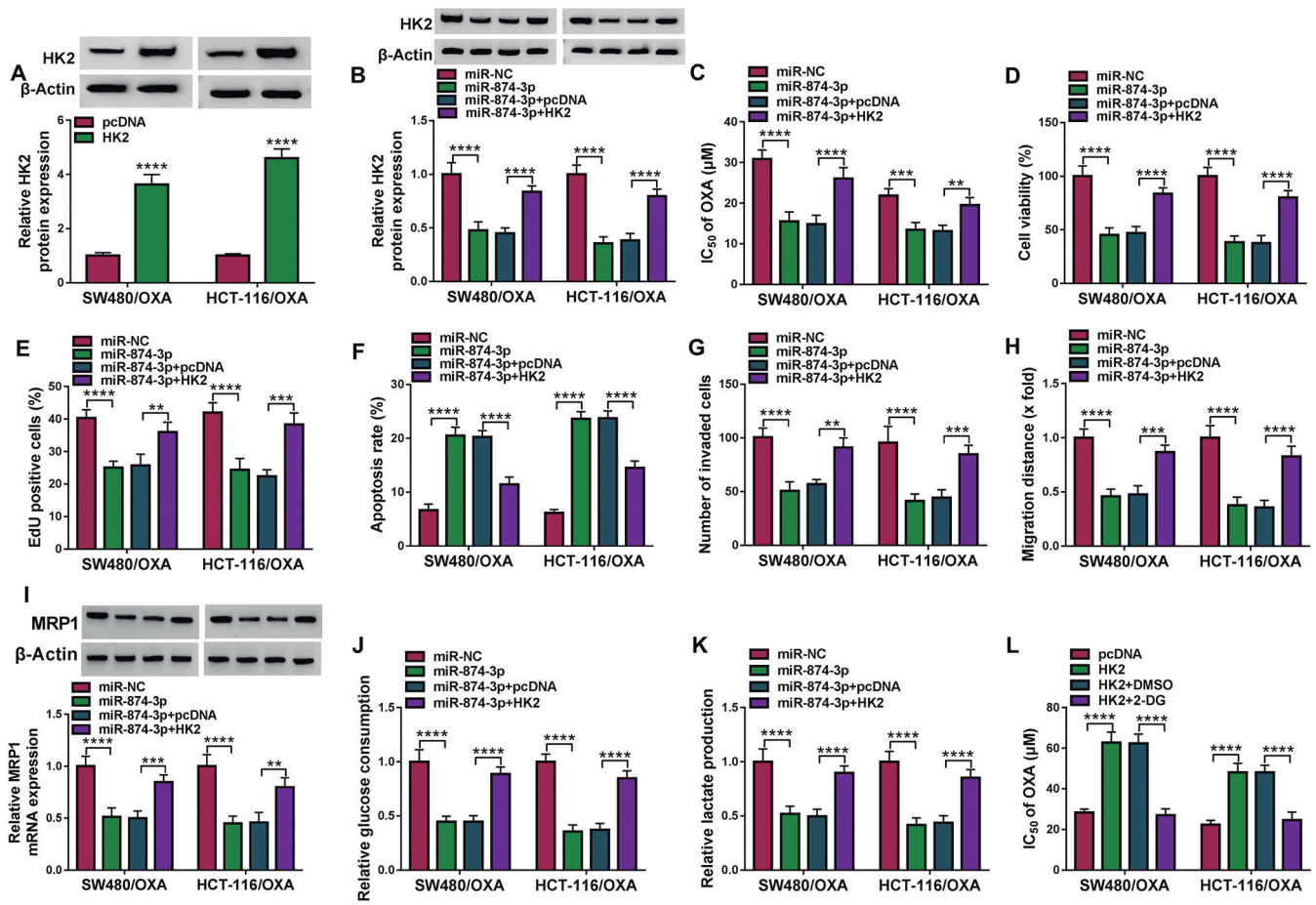

Fig. 9. MiR-874-3p regulated the progression of CRC by targeting HK2. **A, B.** The HK2 contents were detected. **C, K.** The IC_{50} of OXA **(D)** the OD value, the cell proliferation **(E)**, the apoptosis **(F)**, the number of invaded cells **(G)**, the number of migration cells **(H)**, the MRP1 level **(I)**, the glucose metabolism **(J, K)**, The IC_{50} of OXA were assessed **(L)**. ***P*<0.01, ****P*<0.001, *****P*<0.0001.

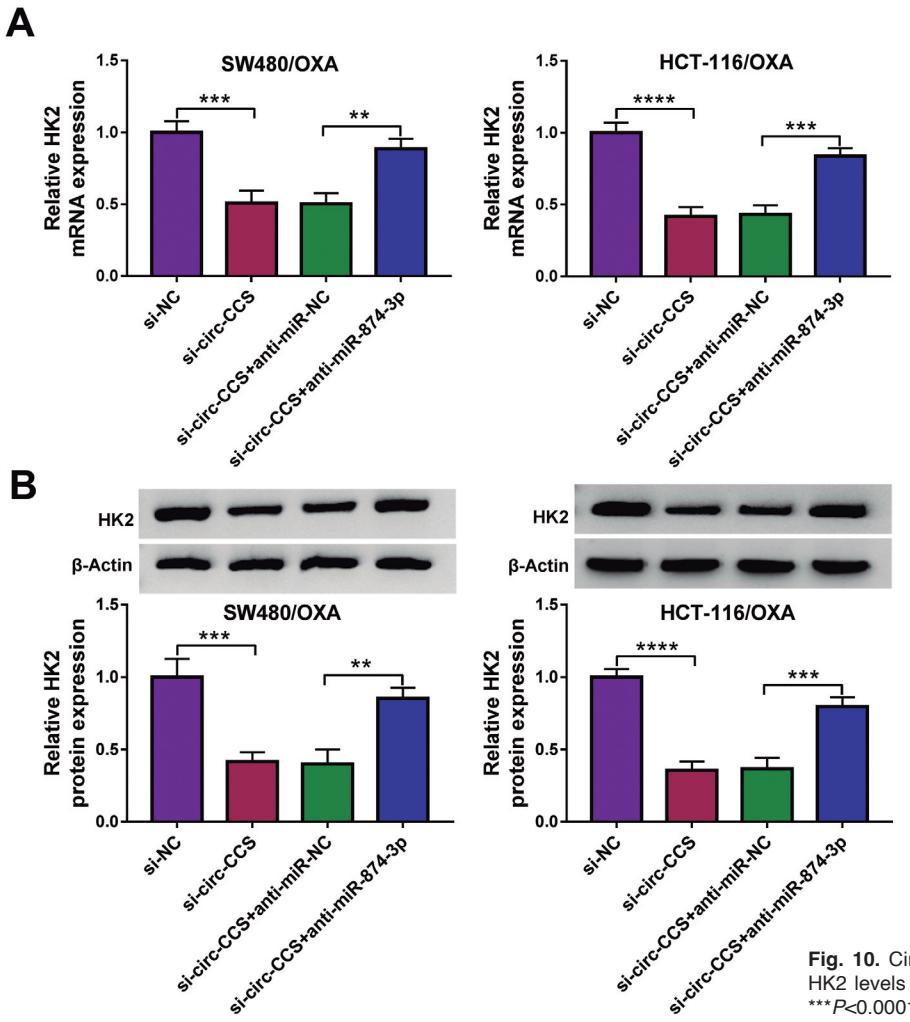

Fig. 10. Circ-CCS regulated HK2 in CRC cells. **A, B.** The HK2 levels were quantified. **P*<0.05. ***P*<0.01, ****P*<0.001, ****P*<0.0001.

3p may participate in CRC development.It was previously reported that miR-513a-5p could prevent glycolysis in CRC cells via curbing HK2 levels (Li et al., 2020). Previous research suggests that the expression of HK2 is frequently higher in a variety of cancer cells (Jin et al., 2014). Besides, the study found that HK2 was strongly associated with overall survival in patients with CRC (Katagiri et al., 2017). In this study, HK2 level was enhanced in CRC. We also demonstrated that miR-874-3p elevated repressed cell IC_{50} value of oxaliplatin, cell vitality, colony formation, migration, invasion and glycolysis metabolism, and this impression was reduced by HK2. We explained that miR-874-3p lack suppressed the inhibiting effect of circ-CCS knockdown on HK2 content in CRC cells. These consequences were a new piece of evidence for the regulatory mechanism of the circ-CCS/miR-874-3p/HK2 in CRC cells. This paper has some significant findings, however, it still has some limitations. For example, the results obtained from commercial cell lines are not completely representative of the actual conditions *in vivo*. The experiment also has no *in vivo* data and clinical statistical support. In the following study, we will implement the experiment to further indicate the part of circ-CCS in clinical application.

Herein, circ-CCS and HK2 were highly expressed and miR-874-3p was lowly expressed in CRC. Furthermore, circ-CCS knockdown suppressed in CRC the IC_{50} value of oxaliplatin, cell vitality, colony formation, migration, invasion and glycolysis metabolism via the miR-874-3p/HK2 axis. We trust that this awareness may deliver a different road for CRC handlings.

Acknowledgements. Not applicable.

Ethics approval and consent to participate. The present study was approved by the ethical review committee of Seventh People's Hospital of Shanghai University of Traditional Chinese Medicine. Written informed consent was obtained from all enrolled patients.

Consent for publication. Patients agree to participate in this work

Availability of data and materials. The analyzed data sets generated during the present study are available from the corresponding author on reasonable request.

Competing interests. The authors declare that they have no competing

interests.

Funding. This work was supported by Science and technology development fund of Pudong, China [PKJ2020-Y15].

References

Ambros V. (2004). The functions of animal microRNAs. Nature 431, 350-355.

Bian L., Zhi X., Ma L., Zhang J., Chen P., Sun S., Li J Sun Y. and Qin J. (2018). Hsa_circRNA_103809 regulated the cell proliferation and migration in colorectal cancer via miR-532-3p / FOXO4 axis. Biochem. Biophys. Res. Commun. 505, 346-352.

Cheng L., Eng C., Nieman L.Z., Kapadia A.S. and Du X.L. (2011). Trends in colorectal cancer incidence by anatomic site and disease stage in the United States from 1976 to 2005. Am. J. Clin. Oncol. 34, 573-580.

Feng X., Xue H., Guo S., Chen Y., Zhang X. and Tang X. (2019). MiR-874-3p suppresses cell proliferation and invasion by targeting ADAM19 in nasopharyngeal carcinoma. Panminerva Med. 63, 238-239.

Gai S., Sun L., Wang H. and Yang P. (2020). Circular RNA hsa_circ_0007121 regulates proliferation, migration, invasion, and epithelial-mesenchymal transition of trophoblast cells by miR-182-5p/PGF axis in preeclampsia. Open Med (Wars). 15, 1061-1071.

Garzon R., Marcucci G. and Croce C.M. (2010). Targeting microRNAs in cancer: rationale, strategies and challenges. Nat. Rev. Drug Discov. 9, 775-789.

Greene J., Baird A.M., Brady L., Lim M., Gray S.G., McDermott R. and Finn S.P. (2017). Circular RNAs: Biogenesis, function and role in human diseases. Front. Mol. Biosci. 4, 38.

Haraldsdottir S., Einarsdottir H.M., Smaradottir A., Gunnlaugsson A. and Halfdanarson T.R. (2014). Colorectal cancer - review. Laeknabladid 100, 75-82 (in Iceland).

Hou W. and Zhang Y. (2021). Circ_0025033 promotes the progression of ovarian cancer by activating the expression of LSM4 via targeting miR-184. Pathol. Res. Pract. 217, 153275.

Jin Z., Gu J., Xin X., Li Y. and Wang H. (2014). Expression of hexokinase 2 in epithelial ovarian tumors and its clinical significance in serous ovarian cancer. Eur. J. Gynaecol. Oncol. 35, 519-24.

Katagiri M., Karasawa H., Takagi K., Nakayama S., Yabuuchi S., Fujishima F., Naitoh T., Watanabe M., Suzuki T., Unno M. and Sasano H. (2017). Hexokinase 2 in colorectal cancer: a potent prognostic factor associated with glycolysis, proliferation and migration. Histol. Histopathol. 32, 351-360.

Li H., Jin X., Liu B., Zhang P., Chen W. and Li Q. (2019). CircRNA CBL.11 suppresses cell proliferation by sponging miR-6778-5p in colorectal cancer. BMC Cancer 19, 826.

Li C., Yu Z. and Ye J. (2020). MicroRNA-513a-3p regulates colorectal cancer cell metabolism via targeting hexokinase 2. Exp. Ther. Med. 20, 572-580.

Liu C., Wang X. and Zhang Y. (2019). The roles of HK2 on Tumorigenesis of cervical cancer. Technol Cancer Res. Treat. 18, 1533033819871306.

Liu W.G., Zhuo L., Lu Y., Wang L., Ji Y.X. and Guo Q. (2020). miR-874-3p inhibits cell migration through targeting RGS4 in osteosarcoma. J. Gene Med. 22, e3213.

Liu J., Zhang J., Hu Y., Zou H., Zhang X. and Hu X. (2021). Inhibition of lncRNA DCST1-AS1 suppresses proliferation, migration and invasion of cervical cancer cells by increasing miR-874-3p expression. J. Gene Med. 23, e3281.

Ma Y., Zha J., Yang X., Li Q., Zhang Q., Yin A., Beharry Z., Huang H., Huang J., Bartlett M., Ye K., Yin H. and Cai H. (2021). Long-chain fatty acyl-CoA synthetase 1 promotes prostate cancer progression by elevation of lipogenesis and fatty acid beta-oxidation. Oncogene. 40, 1806-1820.

Roberts D.J., Tan-Sah V.P., Ding E.Y., Smith J.M. and Miyamoto S. (2014). Hexokinase-II positively regulates glucose starvation-induced autophagy through TORC1 inhibition. Mol. Cell. 53, 521-533.

Ros S. and Schulze A. (2013). Glycolysis back in the limelight: systemic targeting of HK2 blocks tumor growth. Cancer Discov. 3, 1105-1107.

Sheng J.Q., Liu L., Wang M.R. and Li P.Y. (2018). Circular RNAs in digestive system cancer: potential biomarkers and therapeutic targets. Am. J. Cancer Res. 8, 1142-1156.

Thanikachalam K. and Khan G. (2019). Colorectal cancer and nutrition. Nutrients 11, 164.

Wang X., Zhang H., Yang H., Bai M., Ning T., Deng T., Liu R., Fan Q., Zhu K., Li J., Zhan Y., Ying G. and Ba Y. (2020). Exosome-delivered circRNA promotes glycolysis to induce chemoresistance through the miR-122-PKM2 axis in colorectal cancer. Mol. Oncol. 14, 539-555.

Xia B., Lin M., Dong W., Chen H., Li B., Zhang X., Hou Y. and Lou G. (2018). Upregulation of miR-874-3p and miR-874-5p inhibits epithelial ovarian cancer malignancy via SIK2. J. Biochem. Mol. Toxicol. 32, e22168.

Xu M., Chen X., Lin K., Zeng K., Liu X., Pan B., Xu X., Xu T., Hu X., Sun L., He B., Pan Y., Sun H. and Wang S. (2018). The long noncoding RNA SNHG1 regulates colorectal cancer cell growth through interactions with EZH2 and miR-154-5p. Mol. Cancer 17, 141.

Xu H., Liu Y., Cheng P., Wang C., Liu Y., Zhou W., Xu Y. and Ji G. (2020). CircRNA_0000392 promotes colorectal cancer progression through the miR-193a-5p/PIK3R3/AKT axis. J. Exp. Clin. Cancer Res. 39, 283.

Yuan R.B., Zhang S.H., He Y., Zhang X.Y. and Zhang Y.B. (2018). MiR-874-3p is an independent prognostic factor and functions as an anti-oncomir in esophageal squamous cell carcinoma via targeting STAT3. Eur. Rev. Med. Pharmacol. Sci. 22, 7265-7273.

Yuan Y., Zhou X., Kang Y., Kuang H., Peng Q., Zhang B., Liu X. and Zhang M. (2021). Circ-CCS is identified as a cancer-promoting circRNA in lung cancer partly by regulating the miR-383/E2F7 axis. Life Sci. 267, 118955.

Zeng K., Chen X., Xu M., Liu X., Hu X., Xu T., Sun H., Pan Y., He B. and Wang S. (2018). CircHIPK3 promotes colorectal cancer growth and metastasis by sponging miR-7. Cell Death Dis. 9, 417.

Zou T., Duan J., Liang J., Shi H., Zhen T., Li H., Zhang F., Dong Y. and Han A. (2018). miR-338-3p suppresses colorectal cancer proliferation and progression by inhibiting MACC1. Int. J. Clin. Exp. Pathol. 11, 2256-2267.

Accepted November 29, 2022